

In Situ Very-High-Energy Diffraction Studies of Thermal Decomposition of Transition Metal Trifluorides

Julietta V. Rau,* Valerio Rossi Albertini,† Norbert S. Chilingarov, Marco Di Michiel,†† Stefano Colonna,† Ilya N. Ioffe, and Lev N. Sidorov

Department of Chemistry, M. V. Lomonosov Moscow State University, 119899 Moscow, Russia

†Istituto di Struttura della Materia/CNR, Via del Fosso del Cavaliere 100-00133 Roma, Italia

††European Synchrotron Radiation Facility, Polygone Scientifique "Louis Neel", Rue Jules Horowitz, 6-38000 Grenoble, France

(Received October 1, 2002)

The thermal decomposition of transition metal trifluorides MF_3 (M = Mn, Fe, Co) was studied by collecting sequences of very-high-energy (89 keV) synchrotron radiation diffraction patterns. The real-time evolution of the crystal lattices was followed as a function of temperature and it was observed that the transition from MF_3 to MF_2 is generally accompanied by the formation of intermediate short-living phases $–M_2F_5$. One of them $–Co_2F_5–$ is a phase which had never been observed before.

Transition metal trifluorides are used as soft fluorinating agents in different fields of chemistry. Co and Mn trifluorides have long been in use in organic synthesis[1,2] and, by now, an extensive literature on the synthesis of various fluorinated derivatives of organic compounds is available.[3] Examples of application of solid fluorinating agents for the synthesis in situ of platinum and gold fluorides are described in Refs. 4 and 5. Among the latest applications of these compounds is the selective fluorination of fullerenes. For instance, the selective synthesis of $C_{60}F_{36}$ has been successfully performed by the solid-phase reaction between C_{60} and MnF_3.[6] Selective products of the reactions between [60]fullerene and other transition metal trifluorides are reported in Ref. 7.

Despite the wide use of solid fluorinating agents, the mechanism of solid-phase fluorination is not well understood yet. This is partially due to the complicated nature of the reacting system, whose components are often present in several phases. A combination of several techniques can yield more information on such kind of systems. Reliable data on the composition of the gas phase can be obtained by High Temperature Mass Spectrometry (HTMS). Our recent mass spectrometric studies[8,9] led to the conclusion that the action of fluorinating agents is due to atomic fluorine released during their decomposition.

The aim of the present research is the investigation of transformations happening in the condensed phase during the thermal decomposition of MnF_3, CoF_3 and FeF_3 by means of Very-High Energy Synchrotron Radiation diffraction. Preliminary experiments showed that this technique is a powerful tool to study the real-time evolution of crystal structures.[10,11]

Experimental

MnF_3, CoF_3, FeF_3 thin powder samples (all of them 98% nominal purity) were purchased from Aldrich Chemical Co. and were manipulated inside an Ar atmosphere dry box (H_2O = 1 ppm).

The method we used to perform the time-resolved studies on the thermal decomposition of transition metal trifluorides is discussed in detail in previous papers.[11,12] Here we summarise its main characteristics.

Ni capillaries (~5 cm in length) having 100 μm thick walls were used as sample holders. They had been preliminary passivated with F_2 (P = 5 atm, T = 720 K) in order to prevent the interaction between Ni and the trifluoride sample during the heating. Indeed, the NiF_2 layer formed on the surface of the capillary after passivation is rather inert with respect to trifluorides and too thin to produce visible Bragg peaks in the diffraction patterns.

The Ni capillaries filled with the sample were placed in the scattering center of a diffractometer equipped with a read-out image plate detector (Fig. 1). For all samples, prior to heating, a reference spectrum at room temperature was collected. Two different ways were used to carry out the measurements (both preventing the contact of the hygroscopic samples with the air moisture), namely either sealing the capillary or submitting the sample to an Ar flux (3.5 cm^3/min) passing through the capillary. In the former case, the fluorine realised upon heating

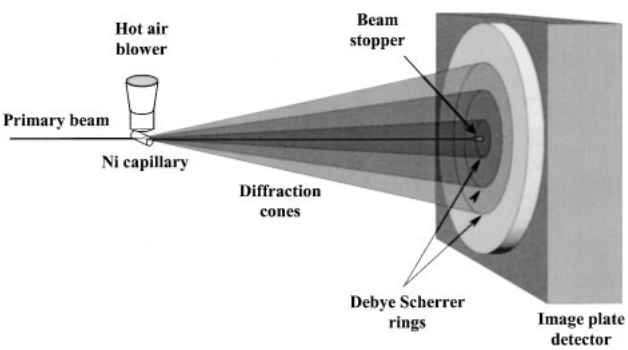

Fig. 1. Sketch of the experimental set-up.

was confined inside the inner volume of the capillary; in the latter, it was rapidly removed by the Ar flux, so that no further interaction with the decomposing sample could happen. In this way, the effect of the F_2 presence during decomposition could be observed by direct comparison of the two cases.

The capillaries were heated at a constant rate by using a hot-air blower. This simplified the experimental set-up and, thanks to the thermal stability of the blower furnace, allowed a very good control of the temperature ramp. Preliminary calibration tests were performed to measure the thermal gradient between the furnace and the sample inside the capillary at any T. After that the capillaries were heated at the rate $\alpha = 1/30$ °C/s. During heating, they were irradiated by the primary X-ray beam with a sampling period of $\Delta t = 70$ s, 10 seconds being the actual collection time, and the remaining 60 seconds being the time required to store the images and to reset the acquisition system. Therefore, the nth pattern of the sequence represents the sample structure at the temperature $T_n \pm \Delta T_n = \alpha n(\Delta t \pm t_0) + T_0$, with $t_0 = 5$ s and $T_0 =$ initial temperature in K. The T-range was from room temperature up to 1370 K. Each experimental run lasted about 9 hours.

At the beginning of each temperature ramp, an acquisition program was launched to collect a sequence of diffraction images. The image-plate detector was automatically read and reset after the collection of each image. The series of the images represent the time evolution of the Debye–Scherrer rings produced by the sample in the various stages of its decomposition process (plus the constant contribution of the capillary walls). By radial integration of the images, the Debye–Scherrer rings were then converted into ordinary diffraction patterns, whose sequence was plotted in the form of a 3D-map (see, for instance, Fig. 2). Each ramp was stopped only after the diffractogram corresponding to the final phase had appeared.

The diffraction measurements were carried out at the high-energy ID15B beamline of the European Synchrotron Radiation Facility (Grenoble, France). The high energy beam is produced by a superconducting wavelength shifter having a critical energy of 95.8 keV. A Bragg monochromator selected a component around the critical energy (at 89 keV in our case) suitable for the diffraction measurement with an energy resolution of 10^{-3}. A slit upstream from the sample collimates the beam, whose final section on the sample is about $100 \times 100\ \mu^2$. The X-ray beam diffracted by the sample is then collected by a MAR345 readout image plate detector centered on the incident beam direction. The use of a 89 keV beam solved completely the problems connected with the X-ray absorption of the metal capillary walls that makes the measurements at lower energies complex and time-consuming. Furthermore, the acceptance solid angle of the image plate detector was so wide that all the low-order Debye–Scherrer rings could be collected, assuring a high statistical accuracy of the diffraction patterns obtained by their radial integration.

Results and Discussion

The time-resolved diffraction studies upon thermal decomposition of manganese, iron and cobalt trifluorides were carried out. In all the three cases, the decomposition process is accompanied by the formation of an intermediate short-living phase of the M_2F_5 kind, while the final product of decomposition is MF_2.

Literature data on solid M_2F_5 compouds are quite limited. Some authors[13] suggested solid Mn_2F_5 to be formed during partial decomposition of MnF_3(s). As a stable phase it was obtained by Tressaud et al.[14] In a recent paper,[10] we reported the observation of MnF_3 thermal decomposition, during which Mn_2F_5 was formed as an intermediate phase. However, the method we applied for that investigation[11] showed some drawbacks and had to be essentially improved to obtain the higher quality data reported in the present paper. Among the other solid M_2F_5 compounds, Fe_2F_5 had been mentioned only in Ref. 15, while Co_2F_5 was first reported by us.[11]

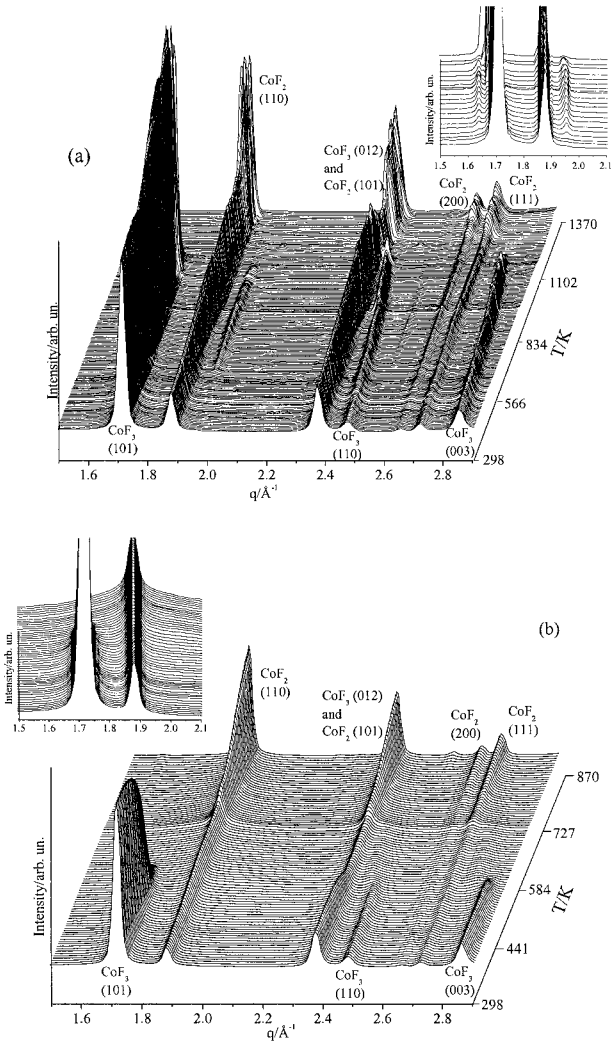

Fig. 2. Sequence of the diffraction patterns acquired upon thermal decomposition of CoF_3: (a) in the sealed capillary; (b) in the capillary submitted to the Ar flux.

The rates of CoF_3, MnF_3, and FeF_3 decomposition are different and the necessity to use Ar flux was conditioned by such differences. For instance, the Co_2F_5 intermediate was observed only in the sealed capillary. Instead, when the capillary was left open and an Ar flux passed through it, the CoF_3 decomposition occurred rather fast and no intermediate was detected. MnF_3 and FeF_3 behave in another way, their decomposition process is slower. To accelerate it and to detect the intermediate compound, it is necessary to remove the released fluorine from the reaction zone by a small Ar flux. The results of the measurements are contained in the sequences of diffraction patterns collected during the sample heating that are

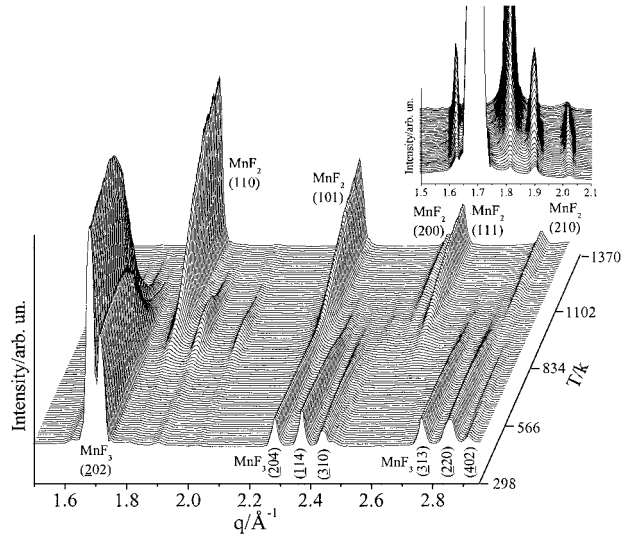

Fig. 3. Sequence of the diffraction patterns acquired upon thermal decomposition of MnF_3.

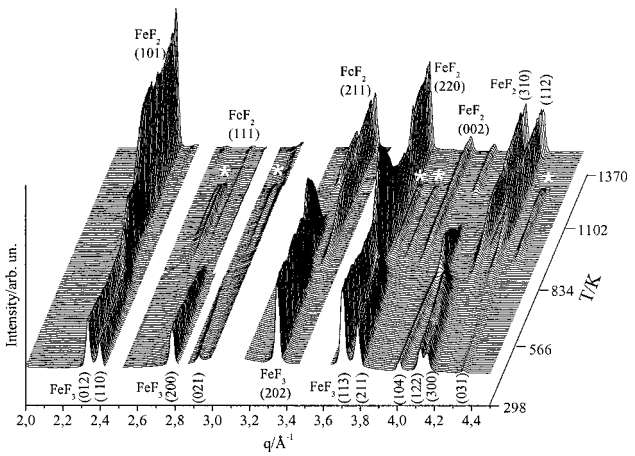

Fig. 4. Sequence of the diffraction patterns acquired upon thermal decomposition of FeF_3. White zones on the graph contain peaks belonging to the sample holder, which were removed to improve the visibility of the graph.

shown in Figs. 2–4 in the form of a 3D-map. It can be seen that for all the three compounds (CoF_3, MnF_3, and FeF_3), the initial phase is the trifluoride and the final phase is the difluoride of the corresponding metal. The peaks of the initial and final phases were assigned according to the International Center for Diffraction Data database.[16]

Figure 2 represents the process of thermal decomposition of CoF_3. In Fig. 2(a), the sequence of diffraction patterns corresponding to the CoF_3 decomposition in the sealed capillary (i.e. without Ar gas flux), is plotted in the momentum transfer range $q = (1.5–2.9)$ Å^{-1}. In Fig. 2(b), the sequence of diffraction patterns corresponding to the CoF_3 decomposition in the capillary submitted to the Ar flux, is shown. In the latter case, the transition occurs directly from CoF_3 to CoF_2 without any intermediate phase. From the comparison of the two 3D-maps, the Bragg peaks produced by the intermediate compound Co_2F_5 are easily identified (at $q = 1.64$ and 1.95 Å^{-1})[11] as can be seen in the insert of Fig. 2(a), where the region $q = (1.5–2.1)$Å^{-1} is magnified. The Co_2F_5 intermediate was observed in the 540–1110 K temperature range. It should be mentioned that low intensity CoF_2 peaks were present already in the first diffractograms taken at room temperature, this was likely due to a small amount of difluoride present in the commercial CoF_3 sample.

The map on Fig. 3 shows the diffraction patterns sequence collected upon thermal decomposition of MnF_3 heated in the capillary submitted to the Ar flux. The peaks of the intermediate Mn_2F_5 phase visible in the T-range 620–1180 K are emphasized in the insert of Fig. 3. Miller indexes of the Mn_2F_5 phase are (400) for the peak at 1.63 Å^{-1}; (220) at 1.90 Å^{-1} and (002) at 2.02 Å^{-1}.[10,14]

In Fig. 4, the sequences of patterns relative to the FeF_3 sample heated in the capillary submitted to the Ar flux are drawn. The Fe_2F_5 intermediate phase (T = 790–1210 K) is marked on Fig. 4 with asterisks. Its Miller indexes[15] are (104) for the peak at $q = 2.63$ Å^{-1} (in our case due to the higher resolution of the technique, it appears to be actually composed by a doublet at 2.63/2.66 Å^{-1}); (204) at 2.95 Å^{-1}; (unindexed) at 3.72 Å^{-1}; (430) at 3.80 Å^{-1}; (325) at 4.38 Å^{-1}. Actually, in the literature,[15] more peaks are reported for Fe_2F_5 phase. In our case it was not possible to observe all the peaks because their position coincided with the positions of more intense peaks of FeF_3 and FeF_2 phases. The small peaks at 3.28 and 4.02 Å^{-1} that appeared at the end of decomposition likely belong to the products of high temperature interaction between fluoride and the sample holder.

The maps corresponding to MnF_3 and FeF_3 heated in the sealed capillaries (not given here) show the same Bragg peaks as on Fig. 3 and 4, but those corresponding to the intermediate.

It is interesting to understand how the transformation from the initial MF_3 structure to the final MF_2 via M_2F_5 takes place. We propose below some speculations concerning this point. It is necessary to stress that we restrict ourselves only to the formal description of a possible model for the phase change processes, which is mainly based on the metal atom sublattice transformations, since the real mechanism of decomposition can be very complex or even stochastic.

In order to clarify the structural transformations in manganese and cobalt fluoride phases, we have reviewed the crystal structures of MF_2, MF_3, and M_2F_5 compounds with M ranging from Cr to Ni in the periodic table reported so far in the Inorganic Crystallographic Structural Database.[17] Among the set of compounds mentioned above, Cr_2F_5 currently remains the only structurally characterized mixed valence phase, while all the di- and trifluoride phases, except for the NiF_3, are well described. The set of transition metal trifluorides as well as the set of difluorides reveal striking resemblances.

Concerning trifluorides, CrF_3, FeF_3, and CoF_3 phases are all trigonal, with very close cell parameters. Only MnF_3 is monoclinic, but can be viewed as slightly distorted trigonal phase. In the trifluorides mentioned above, the metal atoms form almost a simple cubic sublattice and have a slightly irregular octahedral coordination, while fluorine atoms are dicoordinated and form angled (140–150°) M–F–M bridges.

Among the difluoride phases, CrF_2 is monoclinic and represents a minor deviation. It can be similarly regarded as a product of a MnF_2- or NiF_2-like tetragonal phase distortion. In

difluorides the metal atoms exhibit the same octahedral coordination as in trifluorides, though in this case they form a body-centered tetragonal sublattice (distorted in CrF_2), while fluorine atoms become triangularly coordinated.

Since Cr–Ni difluorides are isostructural or almost isostructural, as are the corresponding trifluorides, it seems quite reasonable to suggest the same for the M_2F_5 phases. The assumption that their structures are not significantly different has allowed us to consider the defluorination of CoF_3 and MnF_3 proceeding to difluorides via hypothetic Cr_2F_5-like structures. The almost simple cubic metal atom sublattices in MnF_3 and CoF_3 can be regarded as close packings of tetragonal layers (see Fig. 5(a)). When MnF_3 or CoF_3 phase is transforming into a Cr_2F_5-like structure, those layers undergo parallel shifts along one of the principal axes of an idealized cubic lattice equivalent to the consecutive shifts by ca. 0.4–0.5 of a translation, i.e. closest M–M distance (0.42 in Cr_2F_5), accompanied by a partial loss and rearrangement of fluorine atoms. As the result, the metal atoms split into two distinct classes, referred to as doubly and triply charged. Both of them remain actually octahedrally coordinated; however, the coordination polyhedron for the doubly charged atoms is a highly stretched octahedron, two M–F distances being ca. 25% longer than the remaining four. The metal atom sublattice in this Cr_2F_5-like phase can be described in two different ways: as a system of shifted tetragonal layers, as above, or as a close packing of monoclinic layers perpendicular to the former. Correspondingly, 3/5 of the fluorine atoms in in-layer or near-layer positions remain dicoordinated, while 2/5 of interlayer fluorine atoms can be regarded as tricoordinated due to the presence of a third metal atom at a longer distance (see Fig. 5(b)).

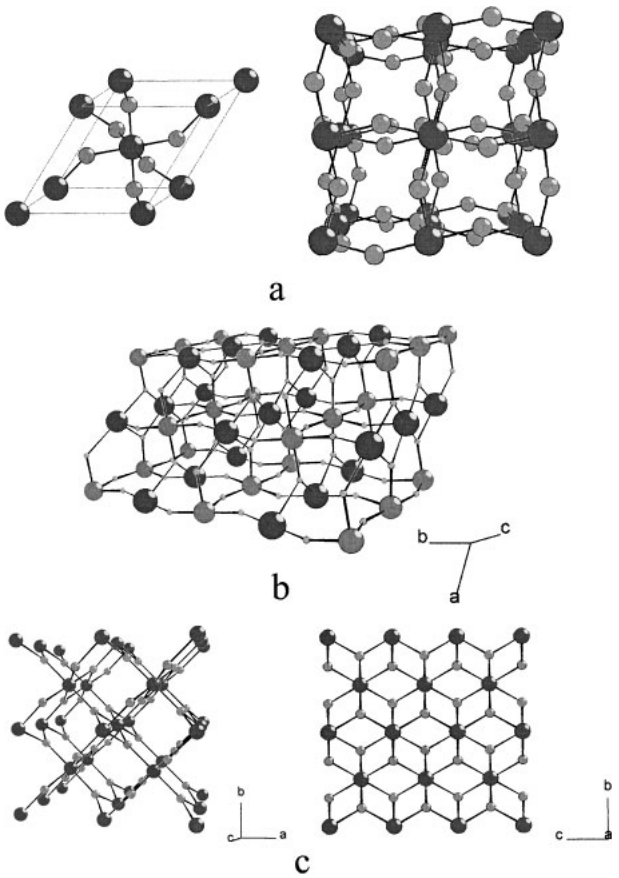

Fig. 5. (a) A unit cell (left) and a projection on the CoF_3 lattice along one of the principal axes of a fictitious simple cubic metal atoms sublattice (dark grey balls: metal atoms, light grey balls: F atoms); (b) A fragment of the Cr_2F_5 lattice. The slightly distorted tetragonal metal atoms layers constitute the ab and bc planes, while the monoclinic (distorted hexagonal) layers form the ac planes (dark grey balls: trivalent Cr atoms, big light grey balls: divalent Cr atoms, small light grey balls: F atoms); (c) Two projections of the CoF_2 lattice.

The body-centered tetragonal metal atom sublattice in MnF_2 and CoF_2 can be described as a tetragonal packing of the metal atoms chains, one half of them (as on a chess board) being shifted by a half-translation along the fourfold axes (see Fig. 5(c)). This arrangement of the metal atoms can be formally obtained from a Cr_2F_5-like structure by an extension of the tetragonal layers shift mentioned above to exactly 1/2 of an in-layer closest M–M distance followed by the shifting of each second monoclinic layer by the same distance and in the same direction. Subsequent partial loss and rearrangement of fluorine atoms lead to the restoration of the equivalence and octahedral coordination of the metal atoms. The same result can be achieved by shifting one-half of the metal atoms chains and rearranging fluorine atoms starting directly from MF_3 phases.

Conclusions

A method based on the in-situ, time-resolved diffraction of high-energy X-rays was applied to study the structural changes occurring upon thermal decomposition of transition metal trifluorides. For CoF_3, the intermediate compound could be observed when the sample-holder (capillary) had been sealed prior to heating. For MnF_3 and FeF_3 the intermediate was detected when the released fluorine was removed from the reaction zone by a small Ar flux.

For MnF_3 and FeF_3, intermediate phases could be identified as the M_2F_5 species, which were already observed in the past, although in different conditions. In the case of CoF_3, the Co_2F_5 had never been observed before, so that this is the first experimental evidence of its existence.

We thank Dr. S.I.Troyanov for his helpful comments. Authors are grateful to Mr. M. Calamita for the technical assistance. We are grateful to European Synchrotron Radiation Facility in Grenoble (France) for the financial support of the experiments. The partial contribution of the Russian Foundation for Basic Research (grant no. 01-03-32523) is also acknowledged.

References

1 M. Stacey and J. C. Tatlow, *Adv. Fluor. Chem.*, **1**, 160 (1960).

2 J. Burdon, I. W. Parsons, and J. C. Tatlow, *Tetrahedron*, **28**, 43 (1972).

3 J. C. Tatlow, *J. Fluorine. Chem.*, **75**, 7 (1995).

4 M. V. Korobov, N. S. Chilingarov, N. A. Igolkina, M. I. Nikitin, and L. N. Sidorov, *Russ. J. Phys. Chem.* (Translated from

Russ. Zh. Fiz. Khim.), **58**, 2250 (1984).

5 N. S. Chilingarov, M. V. Korobov, S. V. Rudometkin, A. S. Alikhanyan, and L. N. Sidorov, *Int. J. Mass Spectrom. Ion Phys.*, **69**, 175 (1986).

6 O. V. Boltalina, A. Ya. Borschevskii, L. N. Sidorov, J. M. Street, and R. Taylor, *J. Chem. Soc., Chem. Commun.*, **1996**, 529.

7 A. A. Goryunkov, V. Yu. Markov, O. V. Boltalina, B. Zemva, A. K. Abdul-Sada, and R. Taylor, *J. Fluorine. Chem.*, **110**, 191 (2001).

8 N. S. Chilingarov, J. V. Rau, L. N. Sidorov, L. Bencze, A. Popovic, and V. F. Sukhoverkhov, *J. Fluorine. Chem.*, **104**, 291 (2000).

9 J. V. Rau, N. S. Chilingarov, M. S. Leskiv, V. F. Sukhoverkhov, V. Rossi Albertini, and L. N. Sidorov, *J. Phys. IV France*, **11**, 109 (2001).

10 J. V. Rau, V. Rossi Albertini, N. S. Chilingarov, S. Colonna, and U. Anselmi Tamburini, *J. Fluorine Chem.*, **108**, 253 (2001).

11 J. V. Rau, V. Rossi Albertini, N. S. Chilingarov, S. Colonna, and M. Di Michiel, *Chem. Lett.*, **2002**, 664.

12 V. Rossi Albertini, P. Perfetti, F. Ronci, P. Reale, and B. Scrosati, *Appl. Phys. Lett.*, **79**, 27 (2001).

13 T. C. Ehlert and M. Hsia, *J. Fluorine Chem.*, **2**, 33 (1972/73).

14 A. Tressaud and J. Dance, *C.R. Acad. Sc. Paris, Ser. C*, **278**, 463 (1974).

15 G. Brauer and M Eichner, *Z. Anorg. Allgem. Chem.*, **296**, 13 (1958).

16 Copyright© JCPDS-International Center for Diffraction Data 1993. Newtown Square Corporation Campus, 12 Campus Boulevard, Newtown Square, Pennsylvania, 19073-3273, U.S.A.

17 Copyright© Inorganic Crystallographic Structural Database. Fachinformationszentrum, Karlsruhe, **1** (2001).